Innovations in applied physics

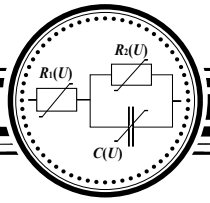

Article DOI: 10.18500/0869-6632-003191

Study of the microstrip planar slow-wave structures for the millimeter-band vacuum microelectronics devices

R. A. Torgashov[1,2] ✉, *A. G. Rozhnev*[1,2], *N. M. Ryskin*[1,2]

[1]Saratov Branch of Kotelnikov Institute of Radioengineering and Electronics of the RAS, Russia
[2]Saratov State University, Russia
E-mail: ✉torgashovra@gmail.com, rozhnevag@gmail.com, ryskinnm@gmail.com
Received 7.05.2025, accepted 9.07.2025, available online 14.07.2025, published 30.09.2025

Abstract. *The aim* of this work is study of high-frequency characteristics of planar meander-line slow-wave structures on dielectric substrates for millimeter-band traveling-wave tubes with sheet electron beams. *The main method* is numerical simulation of electromagnetic wave propagation processes in the mentioned structures using modern three-dimensional fully-electromagnetic finite-element and finite-difference software simulation packages. *Results.* For the microstrip slow-wave structure in addition to the fundamental slow-wave mode there exist fast volume modes, which can prevent stable regimes of TWT-amplifier operation. The spatial parameters of the structure were optimized to suppress the volume modes in the operating frequency band. High values of the attenuation coefficient of the surface slow-wave modes are also the features of the system. The results of the simulation of the ohmic losses using different numerical methods are presented, their qualitative and quantitative comparison is carried out. *Conclusion.* The high-frequency characteristics of miniaturized planar microstrip meander-line slow-wave structures on a dielectric substrate are studied in detail. The effect of spatial parameters of the structure on the cut-off frequencies of volume and surface modes is investigated. The main methods of ohmic loss simulation are presented. It is shown that simulation using perturbation theory and time-domain simulation gives underestimated values of ohmic losses.

Keywords: vacuum microelectronics, planar microstrip slow wave structures, traveling wave tube, dispersion, interaction impedance, attenuation coefficient, numerical modeling of the electromagnetic waves, finite element method.

Acknowledgements. This study was carried out within the framework of the state task of Kotelnikov Institute of Radioengineering and Electronics of the RAS.

For citation: Torgashov RA, Rozhnev AG, Ryskin NM. Study of the microstrip planar slow-wave structures for the millimeter-band vacuum microelectronics devices. Izvestiya VUZ. Applied Nonlinear Dynamics. 2025;33(5): 731–747. DOI: 10.18500/0869-6632-003191

Introduction

One of the most important trends in the development of microwave vacuum electronic devices is their miniaturization. In the late 1980s, a whole scientific field, vacuum microelectronics, was formed at the edge of vacuum and solid-state electronics. Moreover, the term «vacuum nanoelectronics» has now come into use. In our country, one of the pioneers of this scientific field is Academician Yuri Vasilyevich Gulyaev, who presented an overview report on the state of research on the problem of miniaturization conducted in the Soviet Union at the First International Conference on Vacuum Microelectronics in Williamsburg, USA (1988) (see [1]).

Miniature analogues of «classic» electrovacuum devices, such as traveling-wave tube (TWT) and backward-wave oscillator (BWO), are of particular interest due to the prospects of mastering the millimeter and submillimeter (terahertz) frequency ranges [2]. The key requirements for such devices are their low weight and small dimensions, as well as the ability to operate at relatively low operating voltages (less than 10 kV). From this point of view, devices with high-frequency structures in the form of planar microstrip slow wave structures (SWS) on dielectric substrates are promising. Such structures are capable of providing high slow-wave factor values, which makes it possible to shorten the length of the interaction space, which is obviously of fundamental importance for miniaturization. Planar microstrip SWS are spatially developed structures in which interaction with high-aspect-ratio sheet electron beams can be ensured. In addition, their design eliminates the need to form a micro-sized beam tunnels for the electron beam.

The first devices based on such SWS were created back in the 1970s [3]. In the 1990s, at the initiative of Yu.V. Gulyaev, the development of miniature devices with planar SWS on dielectric substrates was started at the Saratov Branch of the V. A. Kotelnikov Institute of Radio Engineering and Electronics of the Russian Academy of Sciences (SBIRE RAS). A team of employees led by N. I. Sinitsyn participated in these studies, including G. V. Torgashov, Y. F. Zakharchenko, A. I. Zhbanov, I. S. Nefedov and others. They proposed and investigated the designs of interdigital, ladder, and meander-line SWS, including the millimeter band ones [4].

In the last decade, research on planar SWS has significantly intensified in different countries (USA, China, India, Great Britain, Germany, Singapore) due to the growing interest in the development of the THz band. The greatest attention is paid to meander-line SWS and its various modifications (see, for example, [5–11]). However, other configurations are also possible, for example, interdigital or coplanar structures [12, 13], ring-shaped structures [14] etc. An overview of the current state of research can be found in recent monographs [15, 16]. In particular, work on this topic was resumed at SBIRE RAS, where, together with the employees of Saratov State University, an original technology for manufacturing microstrip SWS based on laser microtreatment of conductive films several microns thick deposited on a dielectric substrate using magnetron sputtering was proposed [5, 17–19]. The obvious advantages of the developed technology are high manufacturing speed, low cost and the ability to quickly make changes to the design of SWS. In addition, magnetron sputtering makes it possible to apply conductive coatings of relatively large thickness (up to 10 μm). Structures up to the D-band of frequencies (110...170 GHz) were fabricated, and the experimental results are in good agreement with the calculated [19].

Currently, various commercial or freely distributed software packages are usually used to study the high-frequency characteristics of SWS, which implement the numerical solution of Maxwell's equations using finite element or finite difference methods. The most common are COMSOL Multiphysics [20], ANSYS HFSS [21] and CST Studio Suite [22]. They make it possible to obtain a fairly complete picture of the propagation of electromagnetic waves in various, including periodic, systems, to study the structure of fields of various modes and other characteristics. This paper presents the results of a study of the high-frequency characteristics of a microstrip meander SWS for a miniature V-band TWT (50...70 GHz). The results of numerical simulation are presented, the structure of eigenmodes and other high-frequency characteristics of SWS are investigated. Special attention is paid to the correct accounting of ohmic losses, which in the case of thin-film structures is quite a difficult task, even when using modern software packages. A comparison with the results of an experimental study of SWS is also presented.

1. High-frequency characteristics of a meander-line SWS on a dielectric substrate

Let us consider a microstrip structure in the form of a rectangular meander-line on a dielectric substrate in a rectangular waveguide with a cross-section of $a \times b$, the scheme of which is shown in Fig. 1. It is assumed that the substrate with a thickness of h_s is made of quartz ($\varepsilon = 3.75$), and its width is equal to the width of the waveguide. The period and width of the microstrip line were chosen to be $d = 200$ μm and $l = 650$ μm, the width of the microstrip was $w = d/4 = 50$ μm, and the thickness of the conductive layer $t = 1$ μm.

The simulation was carried out using the COMSOL Multiphysics software package (the results of calculating the dispersion characteristics and interaction impedance are in good agreement with the data obtained using the CST Studio Suite and ANSYS HFSS software packages considered in this work). At the first step, it was assumed that the substrate has a thickness of $h_s = 500$ μm and is located in a rectangular waveguide of standard cross-section WR-15 ($a \times b = 3.6 \times 1.8$ mm^2), which corresponded to the size of the structure that was studied experimentally in [5]. In Fig. 2, *a* the results of calculating the dispersion characteristics of SWS i.e. frequency f versus phase per the period of the structure φ are presented. An analysis of the eigenmodes in such a system shows that there are two modes corresponding to a surface slow-wave mode. In the dispersion diagram, the corresponding curves coalesce on the π-type of oscillations. This is due to the fact that the system has a sliding plane of symmetry [23].

The slow wave is the surface mode, which field is localized close to the microstrip line, and the transverse wavenumber is purely imaginary. Fig. 2, *b* shows the dependence of the slow-wave factor $n = c/v_{\text{ph}}$ for forward spatial harmonic in the operating frequency range. It can be seen that a high slow-wave factor is provided, which is 5...9 in the range of 50...70 GHz. Accordingly, synchronizm of the wave with the electron beam is possible at sufficiently low voltages of 2...10 kV. There is no lower cut-off frequency for the surface mode, same as for the homogeneous microstrip line.

In addition to slow surface waves, a hybrid volume mode can also propagate in the operating frequency band. The cut-off frequency of this mode coincides with the cut-off frequency of the volume mode of a homogeneous microstrip line and is determined by the transverse dimensions of the structure. From Fig. 2, *b* it can be seen that the volume mode is fast wave ($n < 1$). Thus, it does not interact with the electron beam. However, in input/output couplers, there may be a partial transformation of the signal into the volume mode, which negatively affects matching. Therefore, it is advisable to increase the cut-off frequency of the volume mode so that it lies above the operating frequency band.

A study of the effect of the transverse dimensions of the system on the cut-off frequencies (frequencies

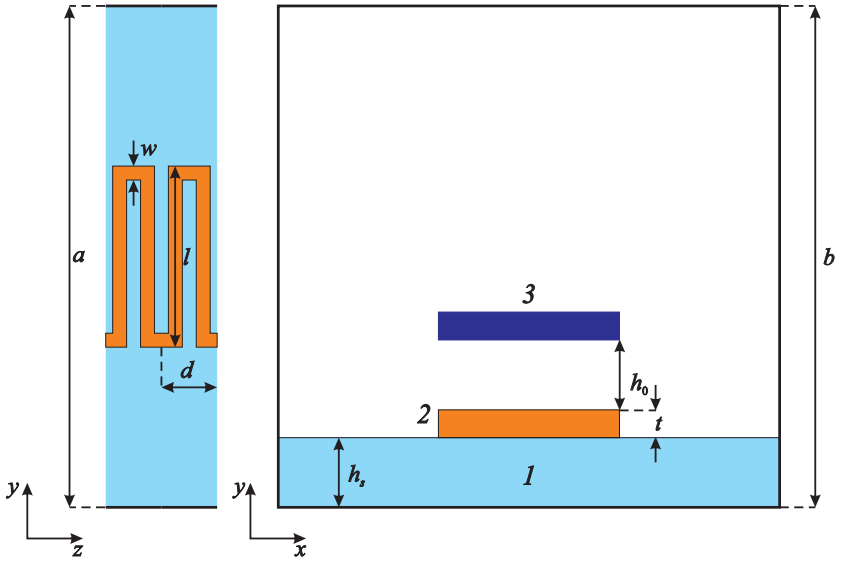

Fig. 1. Schematic diagram of the meander-line SWS on a dielectric substrate: *1* — substrate, *2* — meander line, *3* — electron beam (color online)

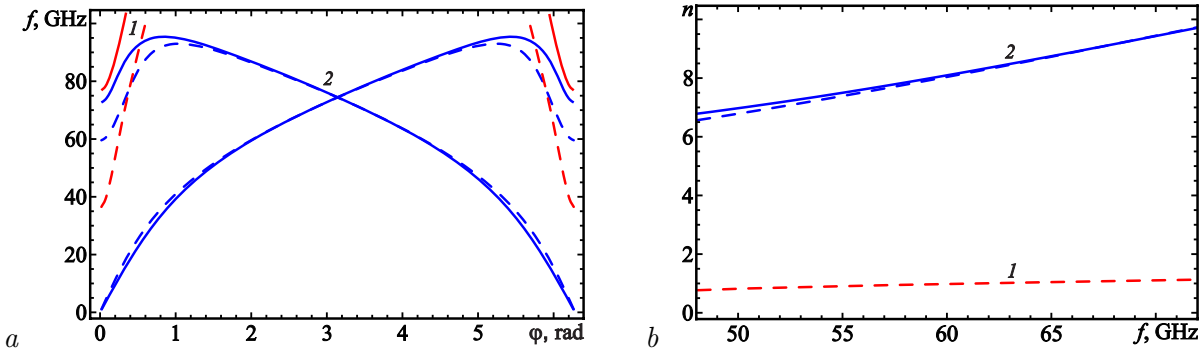

Fig. 2. Dispersion diagram (a) and slow-wave factor vs. frequency (b): *1* — volume fast modes, *2* — surface slow-wave modes. The dashed lines show the dependencies for the original design, the solid lines show those after optimization (color online)

of 2π-type of oscillations) of the volume and surface modes showed that the width of the waveguide and the thickness of the dielectric substrate have the main effect. In Fig. 3 shows the corresponding dependences, from which it can be seen that as the width of the waveguide decreases, the cut-off frequency of the surface slow-wave mode practically does not change, and the cut-off frequency of the volume fast mode increases rapidly. A decrease in the thickness of the substrate leads to an increase in the two indicated frequencies. In this regard, the thickness of the substrate was subsequently reduced to $h_s = 250$ μm, and the width of the waveguide was reduced to $a = 1.8$ mm.

As result of this modification of the geometry the volume mode cut-off frequency increases to 76 GHz and is outside the operating frequency band. At the same time, the dispersion characteristics of the slow-wave mode in the frequency band are 50...70 GHz is changing weakly.

The slow-wave mode also has a pronounced longitudinal component of the electric field, which provides its interaction with the electron beam. An important parameter determining the effectiveness of the beam-wave interaction is the interaction impedance, which is determined by the formula [23, 24]:

$$K_m = \frac{\overline{|E_{z,m}|^2}}{2\beta_m^2 P}\,. \tag{1}$$

Here

$$E_{z,m} = \frac{1}{d}\int_0^d E_z \exp\left(i\beta_m z\right)\, dz \tag{2}$$

is the amplitude of the longitudinal component of the mth spatial harmonic with which the beam interacts,

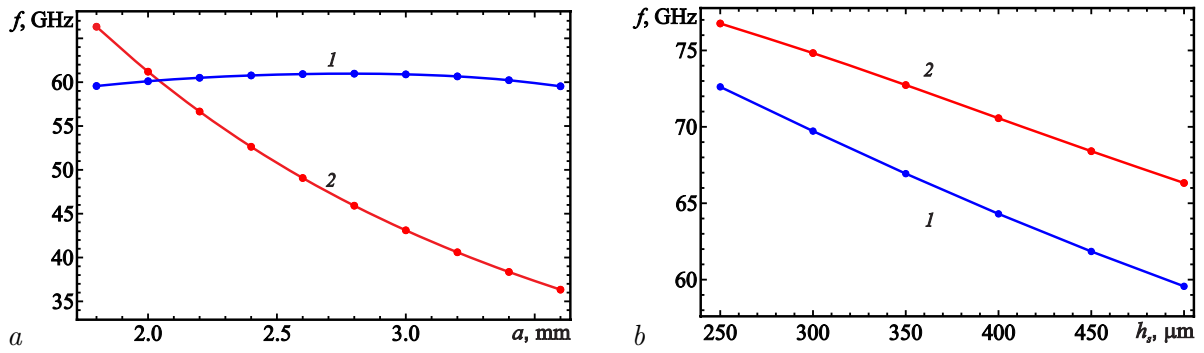

Fig. 3. Frequencies of a 2π–type oscillations vs. waveguide width (a) and substrate thickness (b): *1* — surface slow-wave modes, *2* — volume fast modes (color online)

β_m is the propagation constant,

$$P = \iint\limits_{s_\perp} S_z dxdy = \frac{v_{\text{gr}} W}{d} \tag{3}$$

is a time-averaged power flow through the cross-section of the structure $s_\perp$, carried along the longitudinal direction, S_z is the projection of the Poynting vector onto the longitudinal direction, W is the average time stored energy in the period of the structure, v_{gr} is the group velocity. In (1) the overbar means averaging over the cross-section of the beam S_b:

$$\overline{|E_{z,m}|^2} = \frac{1}{S_b} \iint\limits_{S_b} |E_{z,m}|^2 dxdy\,. \tag{4}$$

Fig. 4 shows the amplitude distribution of the zero spatial harmonic of the slow-wave mode at a frequency of 60 GHz. The spatial harmonic is strongly localized in the area of the meander microstrip structure. Moreover, the amplitude distribution is relatively uniform in the horizontal direction. Accordingly, it is advisable to choose the width of the sheet electron beam that matches the width of the meander.

As you move away from the SWS surface, the amplitude of the spatial harmonic decreases rapidly, varying approximately as $|E_z| \sim \exp(-\gamma_m y)$, where $\gamma_m = \sqrt{{\beta_m}^2 - (\omega/c)^2}$ is the transverse wavenumber. Accordingly, the closer the position of the electron beam is to the surface of the microstrip line, the higher the values of the interaction impedance will be. Also, the beam should have a small thickness. However, sheet electron beams, when focused by permanent magnetic fields, are subject to diocotron instability, which leads to severe deformation of the beam shape as it propagates along the surface of the SWS and creates the risk of electrons settling on the surface of the SWS [25, 26].

Due to the above considerations, the beam size was chosen to be 650×100 μm^2, and it was assumed that the beam propagates at a distance of $h_0 = 75$ μm from the surface of the meander. The position of the electron beam is shown by a rectangle in Fig. 4.

The development of SWS with a higher thickness of the conductive layer t is also of interest, since increasing the thickness reduces the risk of failure owing to current deposition. In Fig. 5 the results of calculating the high-frequency characteristics in the case of an increase in the thickness of the conductive layer to values of 10 μm are presented. It can be seen that with an increase in t, there is a slight change in the dispersion in the operating frequency band (Fig. 5, *a*). The slow-wave factor decreases, as shown in Fig. 5, *b*. The interaction impedance averaged over the beam cross-section in the operating frequency band was also calculated. As can be seen from Fig. 5, *c*, the interaction impedance is quite high, up to 20

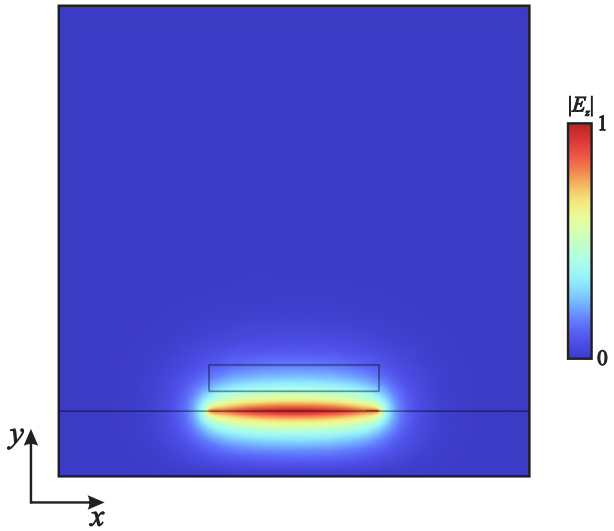

Fig. 4. Distribution of the $|E_{z,m}|$ in the SWS cross section at a frequency of 60 GHz (color online)

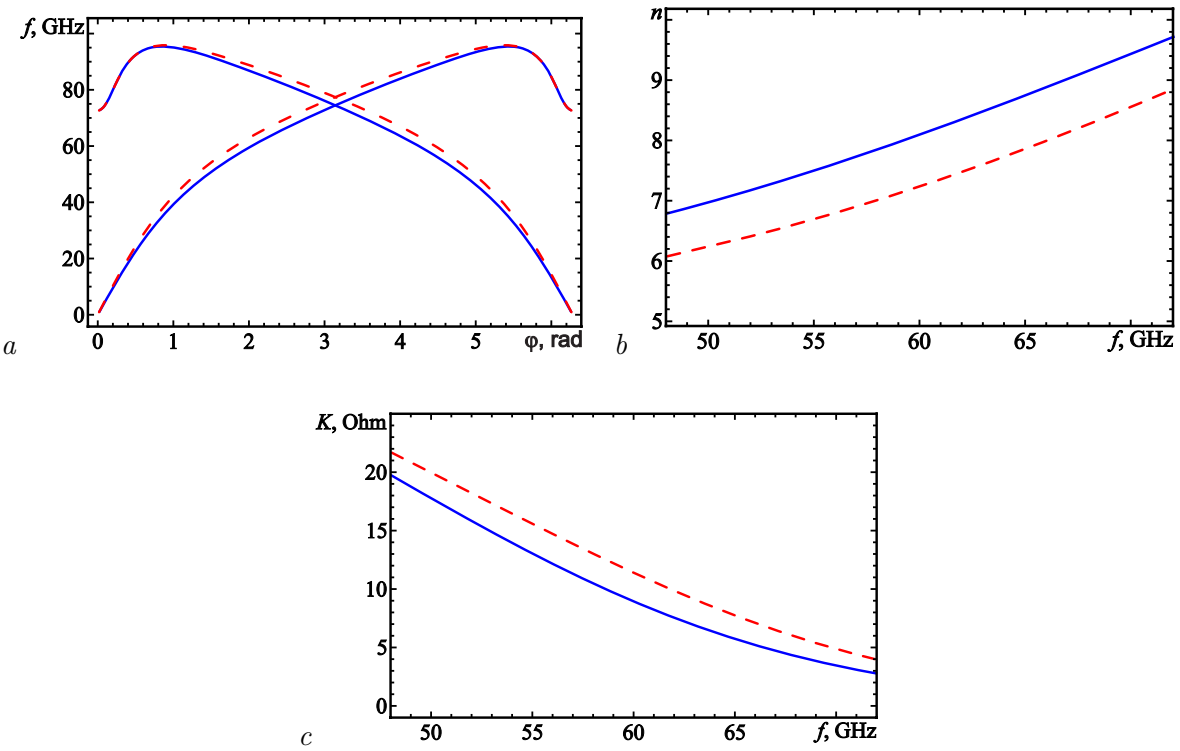

Fig. 5. Dispersion characteristic (a), slow-wave factor (b) and interaction impedance (c) for the SWS with 1-um (solid lines) and 10-um (dashed lines) strip thickness (color online)

Ohm at the long-wavelength end of the operating band. As the frequency increases, its values decrease. An increase in the thickness of the conductive layer leads to an increase in the interaction impedance by about 1.5...2 Ohm in the operating band.

It was shown in [18] that in the V-band TWT with the meander-line SWS with a conductive layer thickness of 10 μm, effective interaction with an electron beam with a current of 100 mA and a voltage of 6 kV is possible. In such a system, high gain values of up to 30 dB can be obtained, as well as an output power of about 15...20 W. The gain band at the level of −3 dB is approximately 2 GHz. These output parameters meet the requirements for millimeter-wave amplifiers for use in next-generation data transmission systems.

2. Features of ohmic losses calculation in thin-film SWS

When designing and developing devices in the millimeter and submillimeter wavelength ranges, an important factor is the correct consideration of ohmic losses, which significantly affect the output characteristics of the devices. In the case of microstrip SWS, additional difficulties arise due to the presence of a thin-film metal coating in the system. The amount of losses increases with decreasing film thickness. This dependence is explained by edge effects, namely, an increase in surface currents flowing through the film near its edges.

Often used methods for accounting for losses due to finite metal conductivity are the use of perturbation theory, as well as impedance boundary conditions (BC) on the metal surface. A limitation of the applicability of these techniques is the requirement that the thickness of the metal layer and the radius of curvature of the surface be significantly greater than the skin depth [27, 28]. The skin depth is calculated using the formula $\delta_s = \sqrt{1/(\pi f \mu\mu_0\sigma)}$, where σ is the conductivity of the metal, μ is its relative magnetic permeability, μ_0 is the vacuum magnetic permeability. For a film made of copper, taking into account the surface roughness, the conductivity lies in the range of $\sigma = (2...3) \cdot 10^7$ S/m. Then, at a frequency of $f = 60$ GHz we get $\delta_s \sim 0.4$ μm, that is, for a film with a thickness of several microns,

the skin depth is a significant fraction of its thickness. In such circumstances, the question arises as to whether these techniques are applicable to millimeter-band systems in the case when the metal film has a small thickness from 1 to 10 μm.

In modern software packages for simulation of electromagnetic fields in various microwave devices, the use of special types of BC is provided, which allow for the modeling of fields in systems containing thin metal elements (films, thin vanes, etc.). For example, COMSOL Multiphysics uses boundary condition. called "Transition Boundary Condition". This BC connects the components of the surface currents flowing along the two sides of a thin film, and through them, the components of the electromagnetic fields at points lying on opposite sides of the film are connected. If the dimensions of the metal elements significantly exceed the thickness of the skin depth, impedance boundary conditions, also implemented in the COMSOL Multiphysics package, work well for modeling systems with ohmic losses.

The ANSYS HFSS (HFSS) code, which is part of the ANSYS Electronics Suite package, uses essentially the same type of BC to model systems with thin metal structures, with the difference that such structures can consist of several layers with different conductivities, which makes it possible to model layered systems or a change in metal conductivity in the direction of normal to its surface.

The CST Microwave Studio (CST), which is an part of the CST Studio Suite and is designed to solve basically the same range of tasks as HFSS, uses either impedance BC to model ohmic losses in metal, as in the two programs mentioned above, or an approach involving the use of perturbation theory. In this case, the system is simulated on the assumption of ideal conductivity of metal elements and the absence of losses in the volume of dielectric inclusions, and then corrections to the frequencies and Q-factor of oscillations in cavity resonators or corrections to the propagation constant and attenuation coefficient are calculated in the case of wave analysis in transmitting structures.

In CST, special macros are implemented to find the characteristics of a system with losses using perturbation theory. Although such features are not available in COMSOL Multiphysics and HFSS, they are easy to implement using the capabilities of the postprocessors of both programs.

In addition, we note that there are two different general approaches to calculating losses in periodic electromagnetic systems. The first is based on simulating the signal transmission through a full-size structure containing a large number of periods and having matching devices at both ends connecting the SWS to regular transmission lines. If the number of periods of the structure is large enough (several dozen or more), and the matching is good, then the contribution of matching elements to the total losses can be neglected. In this case, the attenuation coefficient is determined by the simple formula α [dB/N] $= S_{21}/N$, where S_{21} is an element of the transmission matrix, expressed in dB, N is the number of periods of SWS. The transmission matrix is calculated either in the frequency domain or in the time domain. In the first case, the transmission of a harmonic signal through the system is analyzed, the frequency of which changes to obtain a dependence of the attenuation coefficient in the required frequency band. In another variant, the transmission of a broadband pulse through the system is simulated using a code for non-stationary computer modeling, and then the elements of the transmission matrix of the entire system are calculated using the Fourier transform. Obviously, in both cases, computing devices with powerful processors and large RAM are needed for such calculations. In addition, it takes a considerable amount of time to perform the simulation.

A significantly less time-consuming approach is based on modeling a single SWS cell bounded by two planes perpendicular to its axis and spaced apart by one period d of the structure. Periodic Floquet boundary conditions are set on these planes, according to which fields at two points shifted relative to each other for a period differ only in the phase shift φ, which is set as a parameter. With this formulation, the problem is reduced to calculating the frequencies and Q-factor of eigenmodes of a closed resonator. Due to losses in the metal walls of the SWS and in the volume of possible dielectric inclusions, the eigenfrequencies of the resonator are complex: $\omega_i = \omega'_i + j\gamma_i$, where ω'_i is the real part of the frequency, γ_i is the attenuation coefficient, the index i numbers the types of oscillations. Since the results will be presented below only for the fundamental mode and, accordingly, for the fundamental oscillation in one SWS period, the i index will be omitted.

The found dependence $\omega'(\varphi)$ gives the dispersion law for a wave propagating in the SWS, the value of $\beta = \varphi/d$ is the longitudinal propagation constant. The phase and group velocities are $v_{\text{ph}} = \omega'/\beta$ and $v_{\text{gr}} = d\omega'/d\beta$ respectively. The spatial attenuation coefficient over one period of the SWS α is related to

the time decay rate γ by the relationship $\alpha = \gamma v_{\text{gr}}$. Considering that the Q-factor of the oscillations is

$$Q = \frac{\omega'}{2\gamma}, \tag{5}$$

we obtain the formula for calculating the spatial attenuation parameter in the form

$$\alpha = 8.686 \frac{1}{2Q} \frac{2\pi f d}{v_{\text{gr}}}. \tag{6}$$

The attenuation coefficient here is expressed in dB/period. Formula (6) is convenient in the case of calculations using any of the above-mentioned programs for numerical modeling of electromagnetic fields, since all of them have macros or other capabilities in the postprocessor to calculate the Q-factor of the found eigenmodes in the resonators under study. The group velocity in (6) is determined either by numerical differentiation of the dispersion obtained in the calculation, or by using (3).

The Q-factor of the oscillations in (6), is determined differently depending on the modeling method. If a boundary value problem is solved by setting impedance boundary conditions or transition boundary conditions at the conductive boundaries, and complex permittivity is used to describe absorption in the volume of dielectric inclusions, then the result of calculations will be, among other things, the value of the complex frequency of the calculated mode $\omega = \omega' + j\gamma$. Then the Q-factor is found from formula (5). In the case of the perturbation theory approach, the formula is used to calculate the Q-factor

$$Q = \frac{\omega' W}{\frac{R_s}{2} \int\limits_{S_m} |H_\tau|^2 dS + \frac{\omega'}{2} \int\limits_{V_d} \varepsilon'' \varepsilon_0 \left|\vec{E}\right|^2 dV}. \tag{7}$$

Here $R_s = 1/(\delta_s \sigma)$ is the real part of the surface impedance of the metal, H_τ is the tangent component of the magnetic field to the metal surface, ε'' is the imaginary part of the relative permittivity of volume dielectric inclusions, ε_0 is the dielectric constant, S_m is the surface of the metal with finite conductivity, V_d is the volume occupied by the dielectric.

The described methods for calculating losses and the three software packages mentioned above for numerical simulation of electromagnetic fields are used to calculate the attenuation coefficient in a microstrip planar SWS on a dielectric substrate in a rectangular waveguide. When solving the eigenvalue problem in each of these programs and when modeling a full-size structure in the COMSOL and HFSS software packages, modules implementing the finite element method were used. The calculations were performed on tetrahedral irregular mesh with second-order vector finite elements.

The problem of finding the eigenvalues for oscillations in a resonator in one period of the structure, bounded by planes perpendicular to the axis of the system, on which periodic Floquet boundary conditions were set, was solved. Based on the found frequency values and field distributions, the attenuation coefficient was calculated using the formulas given above. In the course of solving this problem, various software packages used adaptive computational mesh refinement to increase the accuracy of calculating eigenvalues, which led to convergence of the solution after 2–3 iterations. The accuracy of the solution was set using the appropriate solver settings of each program. The relative error was of the order of 10^{-6} for the eigenvalues and $10^{-3}...10^{-4}$ for the calculated fields.

The dimensions of the system were the same as in the previous part of the article. The conductivity used in the calculations was $\sigma = 2.4 \cdot 10^7$ S/m. This value roughly corresponds to the value of the effective conductivity obtained by formula [29]

$$\sigma = \frac{\sigma_0}{\left(1 + \frac{2}{\pi} \arctan\left[1.4\left(\frac{r}{\delta}\right)^2\right]\right)^2} \tag{8}$$

at $f = 60$ GHz, the RMS size of the surface roughness $r = 0.25$ μm and the conductivity of pure oxygen-free copper $\sigma_0 = 5.8 \cdot 10^7$ S/m. The loss tangent of the quartz substrate was loss tangent of $\text{tg}\,\delta = 0.0004$.

Fig. 6 shows the frequency dependences of the attenuation coefficient of the fundamental mode in the studied SWS, calculated using the COMSOL, CST and HFSS packages. The solid lines correspond to the thickness of the film from which the meander is made, equal to 1 μm, the dotted lines are calculated

for 10 μm thick. The blue, red, and green colors are used to represent the results obtained using COMSOL, CST and HFSS, respectively. To calculate the attenuation of structures with a metallization thickness of 10 μm, impedance BC were used in all three cases. At a thickness of 1 μm, the HFSS and COMSOL programs used transition BC and the CST used impedance BC. From Fig. 6 it can be seen that for a thick film, the calculation results for all three programs agree well to each other. At the same time, in the case of a meander with a thickness of 1 μm, the calculation according to the HFSS program gives noticeably lower attenuation values in the high frequency range compared to the other two programs. From Fig. 6 it should also be noted that as the film thickness decreases, the attenuation in the system increases, which is consistent with general theoretical concepts about the impact of edge effects in thin films on the attenuation value.

Next, the question of the possibility of using the perturbation method to calculate attenuation in systems containing thin metal elements was investigated. In Fig. 7 the results of calculating the attenuation coefficient in the meander SWS using two approaches using BC, which explicitly take into account the influence of the finite conductivity of the metal (solid lines), as well as the results obtained using the perturbation method (dotted lines) are presented. The red curves were calculated using CST, and the blue curves were calculated using COMSOL Multiphysics. The thickness of the meander in all cases was 1 μm. To account for the finite conductivity of the metal, transition BC was used in COMSOL, while impedance BC was used in CST. It can be seen from the figure that in the case of thin films, the perturbation method gives significantly underestimated attenuation values compared to more rigorous methods. An additional study also showed that the underestimated values of the attenuation coefficient obtained using the perturbation method are preserved in the case of thicker films, up to a thickness of 10 μm. These results are not given here.

In addition to techniques using single-period simulation, a simulation of signal transmission through a full-size system was also performed and the frequency dependences of the transmission coefficient $S_{21}(f)$ were calculated. After that, attenuation coefficients were obtained as a function of frequency. These results are shown in Fig. 8 where the curve *1* is calculated using the COMSOL Multiphysics program, the curve *2* is calculated using HFSS, and curve 3 is calculated using CST. In the COMSOL and HFSS packages, calculations were performed in the frequency domain using the finite element method, and the CST simulations were performed in time domain by solving three-dimensional Maxwell equations by using the Finite integration technique (FIT), which is a kind of the finite difference time domain method. In the case of HFSS, the SWS model contained 46 SWS periods, while in the other two programs it contained 138 periods.

Curve *4* in Fig. 8 presents the results of an experimental measurement of the transmission coefficient. The measurement procedure is described in detail in [19]. As follows from the figure, the best agreement between the calculation results and experimental data is observed when using the COMSOL Multiphysics

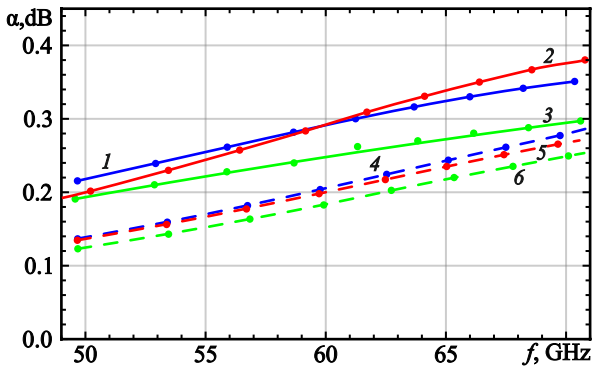

Fig. 6. Attenuation vs. frequency for SWS with metallization thickness of 1 um (solid lines) and 10 um (dashed lines), calculated by various electromagnetic codes: COMSOL (lines *1*, *4*), CST (lines *2*, *5*) and HFSS (lines *3*, *6*) (color online)

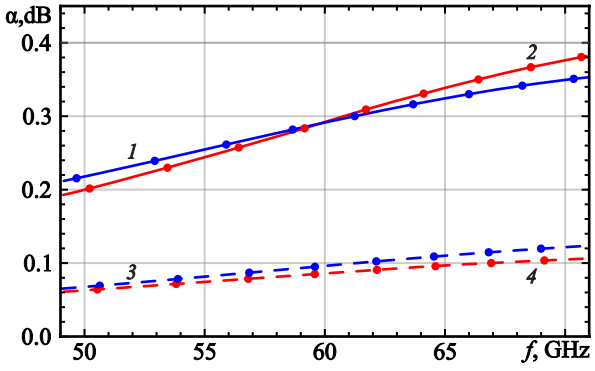

Fig. 7. Comparison of attenuation calculated by COMSOL (lines *1* and *2*) and CST (lines *3* and *4*). *1* and *2* solid lines are calculated by using impedance BC and transition BC on metal surface respectively, dashed lines *3* and *4* are calculated with perturbation theory (color online)

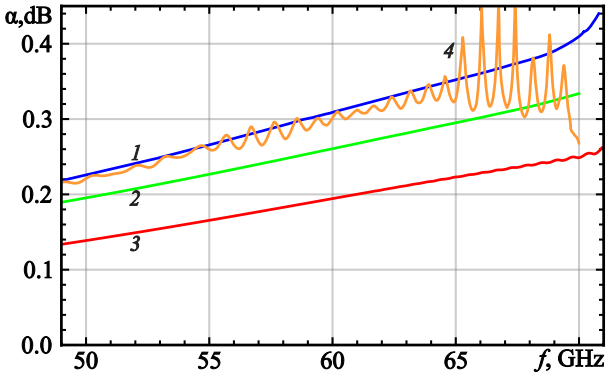

Fig. 8. Comparison of the experimental values of the attenuation vs. frequency with the results of simulation of the full-sized SWS model with metallization thickness of 1 um obtained by COMSOL, HFSS and CST. Line *1* — calculation by COMSOL using transition BC, *2* — by HFSS using transition BC, *3* — by CST using impedance boundary condition in time domain, line *4* — experimental results (color online)

package, where modeling is performed in the frequency domain with the transition BC. The calculation in the time domain using a CST package with impedance BC on thin metal surfaces leads to a significantly lower (almost two times) value of the attenuation coefficient. This circumstance must be taken into account when modeling non-stationary processes of interaction of electromagnetic waves charged particle beams in the case when metal elements with a small thickness are present in the high-frequency structure. To solve such problems, the CST Particle Studio package is often used, in which the part related to the calculation of electromagnetic fields is based on the same algorithms as the CST Microwave Studio program.

When modeling the processes of beam-wave interaction or propagation of electromagnetic waves in the time domain by the finite difference method in the CST software package for the case of SWS with thin metal elements, it is necessary to refine the values of effective conductivity in order to achieve consistency between different methods. As shown in Fig. 6, the calculation of ohmic losses by the finite element method in the frequency domain in the CST and COMSOL software packages gives similar results. Therefore, as a first step, it is proposed to conduct modeling using a single-period model in the CST package, then simulating a full-size model in the time domain with a similar effective conductivity value. If the results show a difference in the calculations of the attenuation coefficient, it is necessary to reduce the effective conductivity value when modeling a full-size model in the time domain in order to achieve consistency in the attenuation value in the system.

Conclusion

The paper provides a detailed analysis of the main high-frequency characteristics of a microstrip slow-wave structure in the form of a rectangular meander on a quartz dielectric substrate for a miniature low-voltage V-band TWT with a sheet electron beam. The structure of dispersion characteristics is investigated. It is shown that, in addition to the fundamental slow-wave mode, a fast volume mode can propagate in the system. The influence of the geometric dimensions of the SWS on the cut-off frequencies of such modes is investigated and the structure is optimized in order to suppress volume modes in the operating frequency-band. It is shown that the surface mode is characterized by high values of the slow-wave factor corresponding to synchronism voltages of the order of 2...10 kV. The structure of the slow-wave mode field is investigated and it is shown that high values of interaction impedance up to 20 ohm are possible in the system, which ensures effective electron-wave interaction in devices such as TWT-amplifiers with such SWS.

It is shown that high values of the attenuation coefficient are characteristic for meander-line structures type on a dielectric substrate. In the process of numerical modeling, careful selection of the method of loss accounting is necessary, since the use of different techniques can lead to very different results. In calculations based on the analysis of eigenmodes in one period of the structure, the most reliable results are those obtained using COMSOL with transition BC, as well as the results of the CST

program using impedance BC. The latter circumstance is unexpected, since the formal conditions for the applicability of impedance BC are not fulfilled for films with a thickness of 1 μm.

The use of perturbation theory formulas in the entire studied range of meander thicknesses of 1...10 μm leads to significant errors in determining the attenuation coefficient SWS.

Time-domain modeling of a full-size system using CST and impedance BC predicts a significantly lower attenuation coefficient compared to experimental data and the results of full-size modeling in the frequency domain using COMSOL. This feature must be taken into account when modeling non-stationary processes in electromagnetic structures containing thin metal elements using CST, in particular, when modeling the interaction of electromagnetic waves with charged particle beams.

References

1. Gulyaev YV, Sinitsyn NI. Super-miniaturization of low-power vacuum microwave devices. IEEE Trans. Electron Devices. 1989;36(11):2742–2743. DOI: 10.1109/16.43782.
2. Denisov GG, Glyavin MYu, Ginzburg NS, Zotova IV, Peskov NY, Savilov AV, Ryskin NM. Vacuum microwave electronics: development of terahertz frequency range. In: Panchenko VYa, editor.Terahertz Photonics and Optoelectronics. M.: RAS; 2024. 764 p. (in Russian).
3. Potter BR, Scott AW, Tancredi JJ. High-power printed circuit traveling wave tubes. In: 1973 International Electron Devices Meeting. 1973, Washington, DC, USA. P. 521–524. DOI: 10.1109/IEDM.1973.188775.
4. Gulyaev YuV, Zhbanov AI, Zakharchenko YuF, Nefedov IS, Sinitsyn NI, Torgashov GV. Planar slow-wave systems for miniature electrovacuum microwave devices. J. Commun. Technol. Electron. 1994;39(12):2049–2058.
5. Ryskin NM, Rozhnev AG, Starodubov AV, Serdobintsev AA, Pavlov AM, Benedik AI, Torgashov RA, Torgashov GV, Sinitsyn NI. Planar microstrip slow-wave structure for low-voltage V-band traveling-wave tube with a sheet electron beam. IEEE Electron Device Letters. 2018;39(5):757–760. DOI: 10.1109/LED.2018.2821770.
6. Wang S, Aditya S, Xia X, Ali Z, Miao J. On-wafer microstrip meander-line slow-wave structure at Ka-band. IEEE Trans. Electron Devices. 2018;65(6):2142–2148. DOI: 10.1109/TED.2018.2798575.
7. Wang S, Aditya S, Xia X, Ali Z, Miao J, Zheng Y. Ka-band symmetric V-shaped meander-line slow wave structure. IEEE Transactions on Plasma Science. 2019;47(10):4650–4657. DOI: 10.1109/TPS.2019.2940254.
8. Wang Z, Du F, Li S, Hu Q, Duan Z, Gong H, Gong Y, Feng J. Study on an X-band sheet beam meander-line SWS. IEEE Transactions on Plasma Science. 2020;48(12):4149–4154. DOI: 10.1109/TPS.2020.3035411.
9. Socuéllamos JM, Dionisio R, Letizia R, Paoloni C. Experimental validation of phase velocity and interaction impedance of meander-line slow-wave structures for space traveling-wave tubes. IEEE Transactions on Microwave Theory and Techniques. 2021;69(4):2148–2154. DOI: 10.1109/TMTT.2021.3054913.
10. Guo G, Zhang T, Zeng J, Yang Z, Yue L, Wei Y. Investigation and fabrication of the printed microstrip meander-line slow-wave structures for D-band traveling wave tubes. IEEE Trans. Electron Devices. 2022;69(9):5229–5234. DOI: 10.1109/TED.2022.3192214.
11. Guo G, Jing Z, Qixiang Z, Tianzhong Z, Taifu Z, Pengyu L, HanBiao T, Yanyu W. Investigation and experiment of a novel chamfered V-shaped microstrip slow-wave structure for W-band traveling-wave tube. J. Infrared Milli. Terahz Waves. 2024;45:629–644. DOI: 10.1007/s10762-024-00994-x.
12. Torgashov RA, Benedik AI, Ryskin NM. Study of miniaturized low-voltage backward-wave oscillator with a planar slow-wave structure. Izvestiya VUZ. Applied Nonlinear Dynamics. 2017;25(5):35–46. (in Russian). DOI: 10.18500/0869-6632-2017-25-5-35-46.
13. Zhao C, Aditya S, Wang S. A novel coplanar slow-wave structure for millimeter-wave BWO applications. IEEE Trans. Electron Devices. 2021;68(4):1924–1929. DOI: 10.1109/TED.2021.3059435.
14. Ulisse G, Krozer V. W-band traveling wave tube amplifier based on planar slow wave structure. IEEE Electron Device Letters. 2017; 38(1):126–129. DOI: 10.1109/LED.2016.2627602.
15. Zhao C, Aditya S. Planar Slow-Wave Structures: Applications in Traveling-Wave Tubes. Institute of Physics Publishing; 2024. 326 p. DOI: 10.1088/978-0-7503-5764-7.
16. Gong Y, Wang S. Planar Slow Wave Structure Traveling Wave Tubes. Design, Fabrication and

Experiment. Institute of Physics Publishing, 2024. 188 p. DOI: 10.1088/978-0-7503-5452-3.
17. Ryskin NM, Torgashov RA, Starodubov AV, Rozhnev AG, Serdobintsev AA, Pavlov AM, Galushka VV, Bessonov DA, Ulisse G, Krozer V. Development of microfabricated planar slow-wave structures on dielectric substrates for miniaturized millimeter-band traveling-wave tubes. J. Vac. Sci. Technol. B. 2021;39(1):013214. DOI: 10.1116/6.0000716.
18. Torgashov RA, Starodubov AV, Rozhnev AG, Ryskin NM. Research and development of traveling Wave tubes with planar microstrip slow-wave structures on dielectric substrates. J. Commun. Technol. Electron. 2022;67:1231–1236. DOI: 10.1134/S1064226922100138.
19. Nozhkin DA, Starodubov AV, Torgashov RA, Galushka VV, Kozhevnikov IO, Serdobintsev AA, Lebedev AD, Kozyrev AA, Ryskin NM. Laser micromachining of 2-D microstrip V-band meander-line slow wave structures. IEEE Trans. Electron Devices. 2025;72(1):453–458. DOI: 10.1109/TED.2024.3507759.
20. RF Module User's Guide, COMSOL Multiphysics® v. 5.6. 2020. Stockholm: COMSOL AB; 2020.
21. High Frequency Structure Simulator (HFSS). ANSYS Inc, Pittsburg, PA, USA [Electronic resource]. Available from: http://www.ansoft.com/products/hf/hfss/
22. CST STUDIO SUITE [Electronic resource]. Available from: http://www.3ds.com/products-services/simulia/products/cst-studio-suite
23. Silin RA, Sazonov VP. Slow-Wave Structures. M.: Sovetskoe Radio; 1966. 632 p. (in Russian).
24. Trubetskov DI, Khramov AE. Lectures on Microwave Electronics for Physicists. Vol. 1. Moscow: Fizmatlit; 2003. 496 p. (in Russian).
25. Cutler CC. Instability in hollow and strip electron beams. J. Appl. Phys. 1955;27(9):1028–1029. DOI: 10.1063/1.1722535.
26. Nguyen KT, Pasour J, Antonsen TM, Larsen PB, Petillo JJ, Levush B. Intense sheet electron beam transport in a uniform solenoidal magnetic field. IEEE Trans. Electron Devices. 2009; 56(5):744–752. DOI: 10.1109/TED.2009.2015420.
27. Vainshtein LA. Electromagnetic waves. Moscow: Radio i Svyaz; 1988. 440 p. (in Russian).
28. Ilìnskiy AS, Slepyan GYa. Oscillations and waves in a electordynamic structures with losses. Moscow: Moscow University Press; 1983. 232 p. (in Russian).
29. Hammerstad EO. Microstrip Handbook / ed. by Bekkadal F. Trondheim, Norway: Norwegian Inst. Technol. Publishing; 1985. 118 p.